Trakya University Journal of Engineering Sciences
http://dergipark.org.tr/tujes
ISSN 2147–0308

Research Article / Araştırma Makalesi
DOI: 10.59314/tujes.1598718

Artificial Neural Network Models of Cross-Linked Polyethylene

Rabia KORKMAZ TAN[1*], Hakan ÇANTA[2], Reşat MUTLU[3]

[1*]*Electronics Department, Vocational School of Technical Sciences, Tekirdağ Namık Kemal University, Tekirdag, Türkiye*

[2]*Unika Cable, Çerkezköy, Tekirdağ, Türkiye*

[3]*Electrical and Electronics Engineering Department, Çorlu Engineering Faculty, Tekirdağ Namık Kemal University, Çorlu, Tekirdağ, Türkiye*

Cite this article as: Korkmaz Tan, R., Çanta, H., Mutlu, R. (2024). Artificial Neural Network Models of Cross-Linked Polyethylene, *Trakya University Journal of Engineering Sciences*, 25(2), 129-141.

Highlights

- Temperature and Frequency Dependent Model of XLPE Permittivity
- Modeling of XLPE Permittivity with ANN
- Performance Optimization of ANN Models

Article Info

Article History:

Received:
December 9, 2024

Accepted:
December 19, 2024

Keywords:

Power cables;
Insulation models;
Cross-linked polyethylene;
ANN model;
Parameter prediction.

Abstract

Cross-linked polyethylene (XLPE) is the most widely used insulator material in high-power cables. The complex electrical permittivity of the XLPE layer mostly determines the leakage admittance of the cable and the propagation speed of the signal. The complex electrical permittivity of XLPE depends on not only operating frequency but also temperature. In this study, Artificial neural networks (ANNs) are used to model the complex electrical permittivity parts of the XLPE. The structure of the ANNs is optimized. It has been found that the optimized ANN can predict the behavior of the XLPE with an R^2 value of 0.99.

Çapraz Bağlı Polietilenin Yapay Sinir Ağı Modelleri

Makale Bilgileri

Makale Tarihçesi:

Geliş:
9 Aralık 2024

Kabul:
19 Aralık 2024

Anahtar Kelimeler:

Yüksek gerilim kabloları;
Yalıtım modelleri;
Çapraz bağlı polietilen;
YSA modeli;
Parametre tahmini.

Öz

Çapraz bağlı polietilen (XLPE), yüksek güçlü kablolarda en yaygın kullanılan yalıtkan malzemedir. XLPE katmanının kompleks elektriksel geçirgenliği, genellikle kablonun kaçak admitansını ve sinyalin yayılma hızını belirler. XLPE'nin karmaşık elektriksel geçirgenliği, sadece çalışma frekansına değil, aynı zamanda sıcaklığa da bağlıdır. Bu çalışmada, XLPE'nin karmaşık elektriksel geçirgenlik bileşenlerini modellemek için çok katmanlı algılayıcılar Yapay Sinir Ağları (YSA) kullanılmıştır YSAların yapısı optimize edilmiştir. Optimize edilmiş YSA'nın XLPE'nin davranışını 0.99 R^2 değeriyle tahmin edebildiği bulunmuştur.

[*]**Correspondence to: rkorkmaz@nku.edu.tr**

1. Introduction

Artificial neural networks (ANNs) are circuits or programs that mimic biological neurons (Haykin, 1998). ANNs are commonly used for classification, modeling, prediction, and estimation (Haykin, 1998; Liang and Bose, 1996). They are also used to model the results of industrial processes (Rajagopalan and Rajagopalan, 1996). Communication and power cables are important components of electrical power systems (Moore, 1997). An ANN is used to predict the characteristic impedance and return loss of a communication cable (Öztürk et al. 2020). Similar ANNs are used to compare the performance of two different cable production machines (Öztürk et al. 2019). XLPE is one of the commonly used insulators in power cables (Thue, 2017). Defects, wetting angle, and water-treeing characteristics of XLPE material are examined to achieve optimal performance in cable applications (Uydur et al. 2018; Karhan and Uğur, 2016; Karhan at al. 2021). XLPE permittivity is not constant (Gouda and Matter, 1992). The frequency-dependent complex permittivity of XLPE can be expressed with the Cole-Cole model (Cole and Cole, 1941). XLPE complex permittivity also depends on the temperature (Du et al., 2016). XLPE complex permittivity data has been presented in detail in (Li et al., 2022). Such data can be used to calculate the leakage admittance of a single-core power cable (Çanta et al., 2024). Parameters of aged XLPE cables have been predicted using ANNs (Ge et al., 2022; Arıkan et al., 2022). XLPE defects can also be detected using ANN (Zhou et al., 2023). Partial discharge in cables has been predicted with ANN in (Dessouky et al., 2014). The thermal behavior of XLPE is predicted using an ANN (Wang et al., 2022). The volumetric moisture content of XLPE cable insulation estimation has been made using electric modulus (Das et al., 2022). Machine learning methods have been applied for the prediction of electrical, thermal, and mechanical properties of XLPE cable insulation (Selvamany et al., 2022; Slimani, et al., 2021; Boukezzi and Boubakeur, 2013).. The UV-aged properties of an XLPE cable insulation have been successfully predicted (Hedir, et al., 25). ANNs can be applied to Polymers and Nanocomposites for prediction, estimation, and classification (Ashok et al., 2024). XLPE cable's life has been predicted using an ANN (Zhang et al., 2020). The dielectric response of an insulator has been estimated by an ANN (Shen, et al., 2021). The study aims to use ANNs to model XLPE complex permittivity instead of using the Cole-Cole permittivity model. Different ANN models of XLPE are optimized for this purpose. ANNs having either one or two outputs with different numbers of hidden layers are tried.

This article is arranged as follows. In the second section, the complex permittivity of XLPE using the measured data is presented. In the third section, an ANN model is made for the complex permittivity of XLPE. This article concludes with the last section.

2. The Complex Permittivity of the XLPE Insulator

The leakage calculation of a power cable requires its complex permittivity data for the calculation of the cable leakage capacitance and conductance (Çanta et al., 2024). Such data must present complex permittivity components as a function of not only frequency but also temperature. The leakage current and the complex permittivity of a prism-shaped XLPE block are examined by varying temperature and frequency (Du et al., 2016). The real and imaginary complex permittivity characteristics of XLPE material given in (Du et al., 2016). are reproduced with Getdata program (https://getdata-graph-digitizer.software.informer.com/) and shown in Figure 1. The real and complex parts of the permittivity of XLPE depend on its operating frequency (f) and temperature (T) as shown in Figure 1. XLPE's complex permittivity, $\varepsilon_{\mathrm{XLPE}}(f,T)$, can be expressed as

$$\varepsilon_{\mathrm{XLPE}}(f,T) = \varepsilon_0(\varepsilon'(f,T) - j\varepsilon''(f,T)). \quad (1)$$

where $\varepsilon'$and $\varepsilon''$is the real and imaginary parts of the relative complex permittivity of XLPE, and ε_0 is the permittivity of free space.

Relaxation models are generally used to describe the dielectric relaxation phenomenon in polymer materials (Cole and Cole, 1941). The Cole–Cole equation given by Kenneth Stewart Cole and Robert Hugh Cole is expressed as

$$\varepsilon^*(\omega) = \varepsilon_\infty + \frac{\varepsilon_S - \varepsilon_\infty}{1+(j\omega\tau)^{1-\alpha}} \quad (2)$$

where α is the power exponent parameter ranging zero to one and allowing the description of different spectral shapes, ε_s and ε_∞ are the "static" and "infinite frequency" dielectric constants, respectively, ω is the angular speed and τ is a dielectric relaxation time constant.

The real and imaginary parts of the complex dielectric constant $\varepsilon^*(\omega)$ are, respectively, given as

$$\varepsilon'(\omega) = real\left(\varepsilon^*(\omega)\right) \quad (3)$$

$$\varepsilon'(\omega) = \varepsilon_\infty + \frac{(\varepsilon_S - \varepsilon_\infty)\left(1+(j\omega\tau)^{1-\alpha} sin(\alpha\pi/2)\right)}{1+2\,(\omega\tau)^{1-\alpha} sin(\alpha\pi/2)+(\omega\tau)^{2(1-\alpha)}} \quad (4)$$

And

$$\varepsilon''(\omega) = imag\left(\varepsilon^*(\omega)\right) \quad (5)$$

$$\varepsilon''(\omega) = \frac{(\varepsilon_S - \varepsilon_\infty)(\omega\tau)^{1-\alpha} cos(\alpha\pi/2)}{1+2\,(\omega\tau)^{1-\alpha} sin(\alpha\pi/2)+(\omega\tau)^{2(1-\alpha)}} \quad (6)$$

The relaxation time constant is temperature dependent but, unfortunately, such a model does not represent the temperature dependence of the insulator explicitly. Even if it is expressed as a function frequency, it is quite difficult to curve-fit such a two-variable function even in MATLAB program, and, sometimes, approximations requiring experience are used for this purpose (Wang et al., 2015). A simpler method is needed for this purpose.

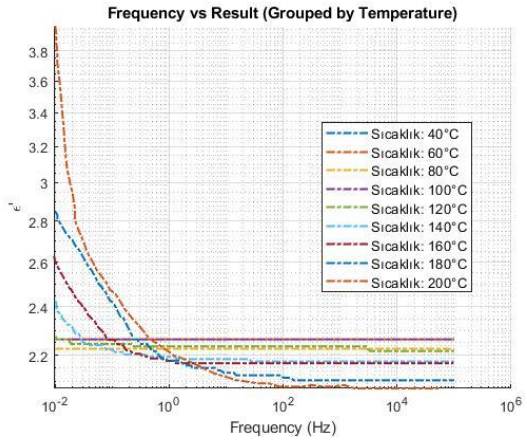

(a)

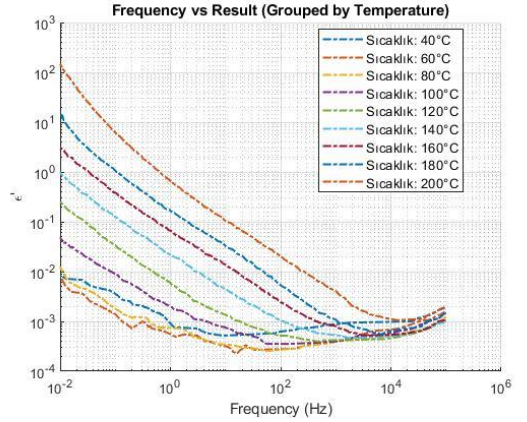

(b)

Figure 1. a) The real part of the complex relative permittivity of XLPE ε' and b) the imaginary part of the relative complex permittivity of XLPE ε'' as a function of the operating frequency and temperature (Du et al., 2016).

3. ANN Models of Complex Permittivity of the XLPE Material

ANNs can be trained to predict the XLPE behavior since ANNs can be used for curve-fitting successfully (Haykin, 1998; Liang and Bose, 1996). In this section, ANN models of the real and imaginary parts of complex permittivity of XLPE material are developed. The Neural Network Toolbox (NNTool) is developed for the MATLABTM program and offers algorithms, pre-trained models and applications to create, train, visualize and simulate shallow and deep neural networks. The NNTool toolbox of MATLAB is used to predict the electrical parameters in this study. Two

separate ANNs are made: the first ANN's output is the real part of the complex permittivity and the second ANN's output is the imaginary part of the complex permittivity as shown in Figure 2. The inputs of all ANNs are the operation temperature and frequency. Both ANNs are optimized by varying the number of ANN layers, the number of neurons in each layer, and the training algorithm type. The structures of the optimized ANNs of the complex permittivity of XLPE and the selection of the number of hidden layer neurons are shown in Figure 3. The ANN has only two hidden layers. In order to reduce the error and obtain the best results, the number of neurons in the hidden layer is set to the values given in Table 1 after the optimization process.

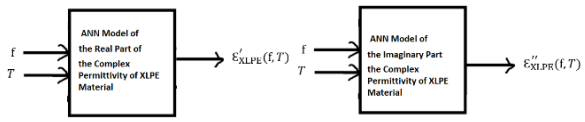

Figure 2. Two ANN models, one with the real part of the complex permittivity as the output and the other with the imaginary part of the complex permittivity as the output

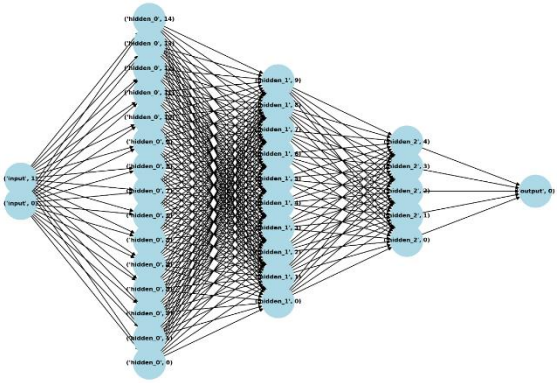

Figure 3. The architecture of the optimized ANNs for each XLPE dataset.

Table 1. The Structure of optimized ANNs

Type Network	Input Layer	1st Hidden Layer		2nd Hidden Layer		Output Layer		Training Algorithm
	Nb. of Neurons	Nb. of Neurons	Activation Function	Nb. of Neurons	Activation Function	Nb. of Neurons	Activation Function	
MLP	2	15	TANSIG	10	TANSIG	5	PURLING	TRINLM

In the artificial neural network (ANN), the sigmoid function is utilized for activation in the hidden layer, while a linear function is applied in the output layer. The NNTool employs the Levenberg-Marquardt (LM) algorithm for weight calculation due to its fast and stable training performance compared to other algorithms. Input data, target outputs, and the data acquisition method (matrix) are specified, along with the distribution percentages for training, validation, and testing datasets. These ratios were adjusted throughout the study to improve results.

This model consists of 3 hidden layers, with 15, 10, and 5 neurons in each layer, respectively as shown in Figure 2. This structure processes the data through different layers and learns complex relationships, enabling the model to make more accurate predictions. As the model progresses from the first hidden layer to the last, the number of neurons decreases. The purpose of designing the model this way is to achieve dimensionality reduction, allowing the model to focus on learning important features. This approach improves the model's ability to generalize, especially when dealing with high-dimensional data.

The visual represents the structure of an artificial neural network with 2 input values and 3 hidden layers. The number of neurons in each layer is as follows:

Input Layer: Composed of 2 neurons. Real data is used at this layer, representing the 2 input features in our data.

First Hidden Layer (Hidden Layer 1): Contains 15 neurons. It processes information from the input layer and passes it to the next hidden layer. The number of neurons in this layer is chosen to transform the input into a more complex representation.

Second Hidden Layer (Hidden Layer 2): Consists of 10 neurons. It further abstracts the information from the first hidden layer, processing it with fewer neurons for more intensive information handling.

Third Hidden Layer (Hidden Layer 3): Has 5 neurons. This layer processes the information from the second hidden layer in a more compact form and passes it to the output layer, facilitating higher-level feature extraction and decision-making.

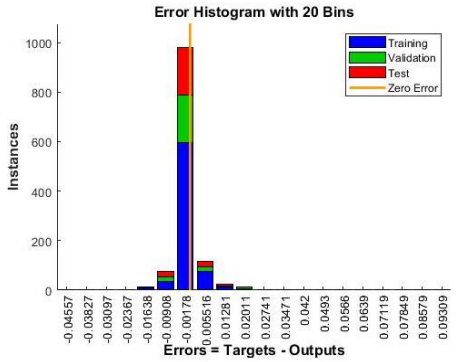

(a)

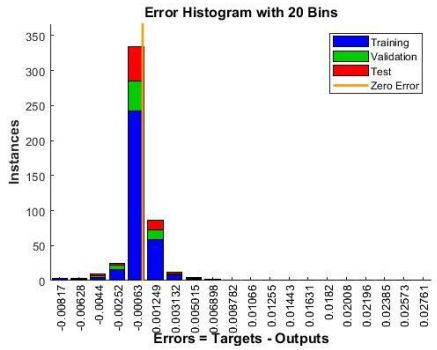

(b)

Figure 4. Error histograms of ANN Models of **a)** the real part (ε′) and **b)** the imaginary part (ε′′) of the complex permittivity of XLPE

Output Layer: Consists of 1 neuron and provides the model's final prediction, usually representing the outcome in classification or regression tasks.

Two error histograms are created to compare the distribution of prediction errors on the model's training, validation, and test datasets as shown in Figure 4. Each graph displays error values using 20 bins, with the frequency of error magnitudes shown on the vertical axis. The values on the horizontal axis represent the difference (error) between target values and predictions.

First Graph (First Visual): In the first histogram, most errors are concentrated around zero, indicating that the model's predictions are quite close to the target values in most cases. The errors for training (blue), validation (red), and test (green) datasets all show high density around zero, with only a small portion deviating from zero. This distribution suggests that the model has generally good generalization and balanced performance across all datasets.

Second Graph (Second Visual): This error histogram displays the distribution of prediction errors for the model on training, validation, and test datasets, divided into 20 error bins. The X-axis represents the error values, calculated as the difference between model outputs and target values, while the Y-axis represents the number of samples within each error bin. Most errors are close to zero, indicating that the model's predictions are generally accurate. The most frequent error range is between -0.4327 and 0.4327, with the majority of errors near zero. Blue bars represent training errors, green bars represent validation errors, and red bars represent test errors, indicating consistent performance across all datasets. The orange line at zero represents perfect predictions, and the small spread around this line shows that the model avoids large errors, demonstrating good performance.

Figure 4 compares the error values (Mean Squared Error - MSE) during the model's training process, illustrating the model's performance across different epochs. In both graphs, the blue line represents training error, the red line represents test error, and the green line represents validation error, while the best validation performance is indicated at the top of each graph.

Best Validation Performance of XLPE Ɛ' Graph: In this graph, the model achieves its best validation performance at the 9276th epoch, with an MSE of 8.1739e-05. Initially, the training, validation, and test errors are at a high level, but as the number of epochs increases, these values continuously decrease. After a certain epoch, significant reductions in validation and test errors are observed, especially between epochs 6000 and 9000, where validation performance improves. This indicates that the model has achieved sufficient generalization capability and is performing well.

Best Validation Performance of XLPE Ɛ" Graph: This graph shows how the MSE values for training, validation, and test datasets change over 10,000 epochs. The Y-axis represents the MSE on a logarithmic scale, while the X-axis represents the number of epochs in the training process. The graph indicates that the model reaches its best validation performance at the 10,000th epoch, with an MSE of 0.61251. Initially, the error is high for all datasets, but as the number of epochs increases, the MSE values gradually decrease, and the model's performance improves. The flattening of the curves suggests that, beyond this point, further learning yields limited performance gains. This indicates that the model has reached the lowest error level on the validation set and that the training process has successfully been completed.

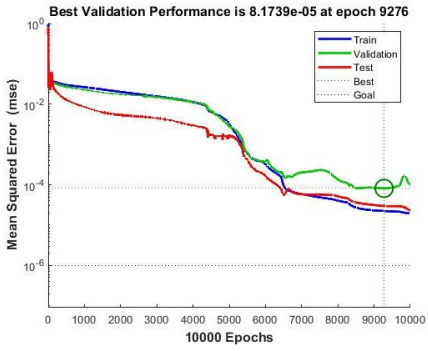

(a)

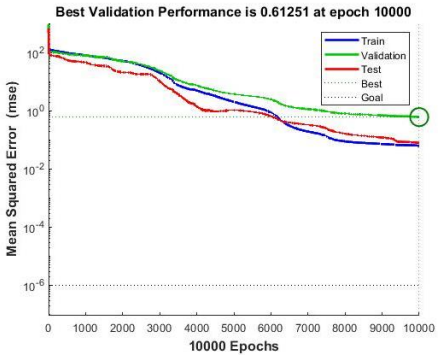

(b)

Figure 5. Best Validation Performance of ANN Models of **a)** the real part (Ɛ′) and **b)** the imaginary part (Ɛ′′) of the complex permittivity of XLPE

Figures 5 compares the error values (Mean Squared Error-MSE) during the model's training process, illustrating the model's performance across different epochs. In both graphs, the blue line represents training error, the red line represents test error, and the green line represents validation error, while the best validation performance is indicated at the top of each graph.

Best Validation Performance of XLPE Ɛ' Graph: In this graph, the model achieves its best validation performance at the 9276th epoch, with an MSE of 8.1739e-05. Initially, the training, validation, and test errors are at a high level, but as the number of epochs increases, these values continuously decrease. After a certain epoch, significant reductions in validation and test errors are observed, especially between epochs 6000 and 9000, where validation performance improves. This indicates that the model has achieved

sufficient generalization capability and is performing well.

Best Validation Performance of XLPE Ɛ" Graph: This graph shows how the MSE values for training, validation, and test datasets change over 10,000 epochs. The Y-axis represents the MSE on a logarithmic scale, while the X-axis represents the number of epochs in the training process. The graph indicates that the model reaches its best validation performance at the 10,000th epoch, with an MSE of 0.61251. Initially, the error is high for all datasets, but as the number of epochs increases, the MSE values gradually decrease, and the model's performance improves. The flattening of the curves suggests that, beyond this point, further learning yields limited performance gains. This indicates that the model has reached the lowest error level on the validation set and that the training process has successfully been completed.

Figure 6 demonstrates how well the model's predicted outputs align with the target values across training, validation, test, and overall datasets. Each graph displays target (actual) values on the horizontal axis and the model's predicted output values on the vertical axis. A black dashed line (Y = T), representing the ideal relationship between outputs and targets, is overlaid with colored lines showing the linear fit of the model's predictions.

For the training data, the R values (correlation coefficients) are found to be 0.99995 and 0.99956, indicating that the model's predictions are very close to the targets. The blue line shows that the model's outputs almost perfectly overlap with the actual targets.

For the validation data, the R values are 0.9998 and 0.99846, demonstrating that the model generalizes well on the validation data, accurately predicting target values without overfitting. The green line also nearly coincides with the targets.

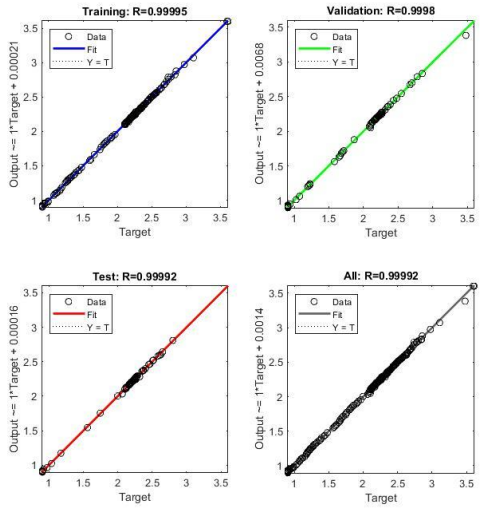

(a)

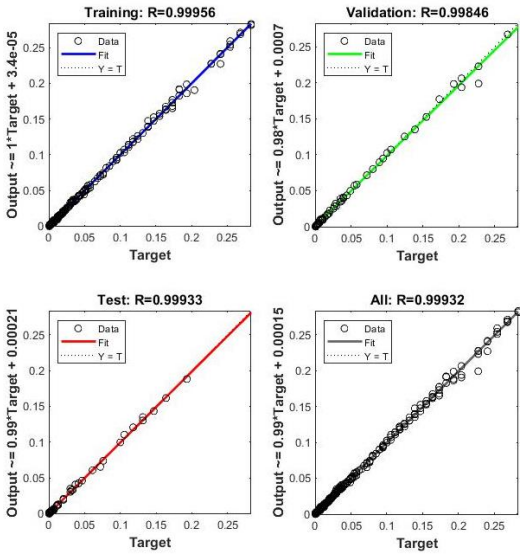

(b)

Figure 6. Regression curves of ANN Models of **a)** the real part (Ɛ′) and **b)** the imaginary part (Ɛ′′) of the complex permittivity of XLPE

For the test data, the R values are 0.99992 and 0.99933, showing that the model performs well even on unseen data. This indicates that the model has strong generalization capabilities and can make consistent predictions across different datasets.

Finally, both figures include a fourth graph, which provides a general analysis of the entire dataset, with R values calculated as 0.99992 and 0.99932. This result shows that the model establishes a strong linear relationship across the entire dataset. The high

agreement between predictions and actual values in all graphs suggests that the model performs well and accurately predicts the targets.

In summary, the model demonstrates strong performance, as evidenced by the high R values and the close alignment between predicted outputs and target values in each graph.

According to the graph, the factors affecting the error bars are as follows: in the top graph, the gradient values initially exhibit high fluctuations but gradually decrease and stabilize over time, indicating that the model encountered optimization issues during the learning process but later began to improve. In the middle graph, the Mu parameter starts at high values and decreases over time, showing that the model achieved more stable learning through adaptive optimization. In the bottom graph, the Validation Checks increase consecutively, indicating that the validation error rises at certain epochs, suggesting a risk of overfitting. This parameter helps detect overfitting and allows the model to stop early. These factors reveal how learning rate, model complexity, and data distribution impact the training process.

Figure 7 compares the model's state during the training process over 10,000 epochs. Each set consists of three sub-graphs: the first graph shows the gradient magnitude, the second graph displays the "Mu" parameter (adaptation parameter), and the third graph presents the number of validation checks.

Neural Network Training State of XLPE Ɛ' Graph: In the first set of graphs, the gradient value at the end of 10,000 epochs is recorded as 0.084. Although the gradient values fluctuate throughout the training process, there is an overall downward trend. This indicates that the model is gradually approaching the lowest error level and is being optimized. In the second graph, the "Mu" value decreases to 10e-7, signifying that the model is entering a more refined learning phase by reducing the adaptation rate. In the third graph, the number of validation checks is 724, indicating that the model failed to maintain improvement on the validation set several times during training. This suggests some fluctuations in validation performance, but the model is generally stable.

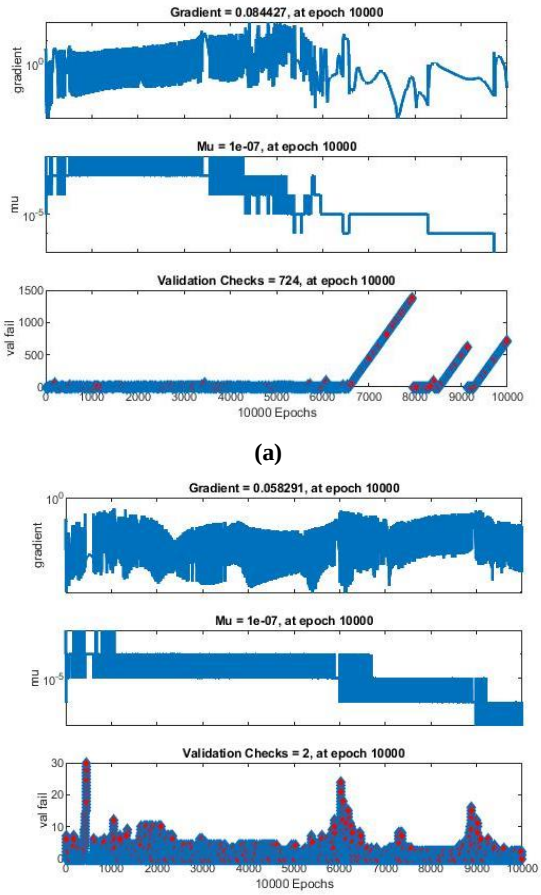

Figure 7. Neural Network Training State of ANN Models of **a)** the real part (Ɛ′) and **b)** the imaginary part (Ɛ′′) of the complex permittivity of XLPE

Neural Network Training State of XLPE Ɛ" Graph: This graph shows the changes over time of three main metrics (gradient, Mu, and validation checks) during the training process of a neural network. The gradient plot determines the update speed of model parameters, and values fluctuating between 10^{-1} and 10 indicate that learning is progressing in a controlled and stable manner. The low range of gradients suggests that the model avoids making excessively large updates. In the middle plot, the Mu (adjustment factor) values, which start at a higher level 10^{-5} to ensure stability during

optimization, gradually decrease to a smaller value 10^{-7}. This reduction shows that the model continues learning with finer, smaller steps.

The bottom plot of validation checks monitors the model's performance on validation data. Only two early stopping checks occurred, indicating that validation loss generally decreased steadily or fluctuated minimally. This suggests that the model is well-adapted to the validation data and avoids overfitting. Overall, the graphs indicate that the model undergoes a stable and controlled training process.

The Coefficient of Determination (R^2) is a measure that indicates how much of the variance in the dependent variable is explained by the model. It takes values between 0 and 1. If the R^2 value is close to 1, the model fits the data very well, and the relationship between the variables is strong. If it is close to 0, the model is insufficient in explaining the data. The R^2 value is generally used in regression models and is important for evaluating the model's generalization capability.

Mean Absolute Deviation (MAD) represents the average of the absolute deviations between predicted values and actual values. This metric is used to evaluate the magnitude of prediction errors. Small MAD values indicate that the model's predictions are close to the target values. MAD is interpreted through the mean for easy understanding of the error amount.

Mean Squared Error (MSE) is the average of the squared differences between predicted values and actual values. Squaring the differences penalizes larger errors more, making the model more sensitive to minimizing errors. Small MSE values indicate a high accuracy of the model's predictions.

Mean Absolute Percentage Error (MAPE) represents the average of the absolute errors between predicted values and actual values as a percentage. It is used to evaluate the model's prediction performance in percentage terms. The lower the MAPE value, the more accurate the model's predictions are.

RMSE (Root Mean Squared Error) is obtained by taking the square root of the MSE and it expresses the magnitude of prediction errors in the original units. RMSE allows for a direct interpretation of the error amount and is sensitive to large errors. Small RMSE values indicate that the predictions are close to the target values.

These concepts are widely used, especially in regression analysis and for evaluating the performance of predictive models such as artificial neural networks. The regression analysis results of this study are presented in Table 2 and Table 3.

The R^2 value for the training set is 0.979, indicating that the model explains 97.9% of the variance in the target variable. This high R^2 value shows that the model fits the training data well and that the learning process has been effective. The low MAD (0.000919) and MSE (5.99e-06) values indicate that the model’s error rates are very low and that predictions are generally close to the target values. Additionally, the MAPE value is as low as 0.041%, reflecting the model’s relatively high accuracy and strong predictive performance on the training data.

The R^2 value for the validation set is 0.994, suggesting that the model can generalize the features learned during training to the validation data effectively. The low MAD (0.002174) and MSE (1.05e-05) values indicate that the model’s predictions on the validation data are close to the targets, with no signs of overfitting. Although the MAPE value is slightly higher than that of the training set at 0.098%, it is still quite low, indicating high relative accuracy on the validation data.

For the test set, the R^2 value is 0.9998, demonstrating that the model can make highly accurate predictions on new, unseen data. However, the MAD (0.004514) and RMSE (0.008947) values are slightly higher than those

of the training and validation sets, indicating larger errors in some test examples. Although the MAPE value is 0.273%, which is slightly higher than the other datasets, it remains low and reflects good relative accuracy. The high R^2 and low error rates indicate that the model has strong generalization capability on the test set as well.

The R^2 value for the training set is 0.998, indicating that the model explains approximately 99.8% of the variance in the target variable. This suggests that the model fits the training data well and has learned the data effectively. The low MAD (0.000933) and MSE (0.5E-05) values show that most of the model's errors are small. However, the high MAPE in the training set suggests that there are relative errors in some cases, though overall performance remains strong.

For the validation set, the R^2 value is as high as 0.934, indicating that the model generalizes well during training. The low MAD (0.002673) and MSE (2,07E-04) values show that the model's predictions on the validation set are also close to the target values. The MAPE is lower than in the training set, indicating relatively higher accuracy.

In the test set, the R^2 value is 0.996, which is very high, indicating that the model makes accurate predictions on previously unseen data. However, the MAD (0.002673) and RMSE (0.003394) values are higher compared to the validation and training sets, suggesting larger errors in some test examples. Nevertheless, the MAPE value is lower than in other datasets, indicating relatively better accuracy.

Table 2. The Performance of single output ANNs for the data of ε'

Set (ε')	**R^2**	**MAD**	**MSE**	**MAPE (%)**	**RMSE**
Training	0,979884	0,000919	5,99E-06	0,040982	0,002448
Validation	0,994232	0,002174	1,05E-05	0,098213	0,003245
Test	0,999806	0,004514	8,01E-05	0,273253	0,008947

Table 3. The Performance of single output ANNs for the data of ε''

Set (ε'')	**R^2**	**MAD**	**MSE**	**MAPE (%)**	**RMSE**
Training	0,998624	0,000933	0,5E-05	12,3593	0,002234
Validation	0,934651	0,002673	2,07E-04	17,8101	0,014382
Test	0,996515	0,002673	1,2E-05	22,8482	0,003394

The high RMSE indicates that the model's predictions in some test instances show larger deviations, though overall performance remains high.

The calculated MSE (Minimum Square Error), R^2 (Regression), and MAPE values of the components of Complex permittivity. Lewis classifies ANN models with their MAPE value as follows (Lewis, 1982).

- If they have a MAPE value lower than 10%, they are 'very good'.
- If they have a MAPE value between 10% and 20%, they are 'good'.
- If they have a MAPE value between 20% and 50%, they are 'acceptable'.
- If they have a MAPE value higher than 50%, they are 'wrong and inaccurate'.

The accuracy of the ANN prediction can be seen in Tables 2 and 3. The low MAPE values obtained and given in Tables 2 and 3 indicate that the deviation between the actual data and the forecast data is small. However, the ANN model for the data of ε'' has a lower performance than the ANN model for the data of ε'.

4. The Conclusion

In this study, the complex permittivity of XLPE material is predicted using ANNs. Using an ANN allows easy interpolation of the complex permittivity components of XLPE without the difficulty of curve-fitting of the complex Cole-Cole models. Levenberg-Marquardt method is used in the training of the ANN. A sigmoid function is chosen as the activity function of the perceptrons. A different ANN is used to model each component of the complex permittivity.

It has been found that A three-layer ANN has given better results than a two-layer ANN in the optimization process.

The error in the predicted cable parameters was calculated based on mean absolute percent error (MAPE). The ANN model of the real part of the complex permittivity of XLPE gives a maximum error of 0.273253% while The ANN model of the imaginary part of the complex permittivity of XLPE gives a maximum error of 22.8482%.

ANN usage in modeling XLPE can make modeling of insulators easier without resorting to the well-known permittivity models such as the Cole-Cole, Maxwell-Wagner, Bruggeman, Rosenkranz, Turner, and Stogryn models. The experience gained here can also be used for modeling other types of power cable insulators.

Author Contributions

Declaration of Competing Interest

The authors declared no conflicts of interest concerning the research, authorship, and/or publication of this article.

Acknowledgments

This study has been supported by the research and development center of Ünika Üniversal Kablo Sanayi ve Tic. A.Ş.; Project number: **UPN-2003.**

ORCID

Rabia Korkmaz Tan, 0000-0002-3777-2536
Hakan Çanta, 0009-0004-2013-1478
Reşat Mutlu, 0000-0003-0030-7136

References

Arikan, O., Uydur, C. C., & Kumru, C. F. (2022). Prediction of dielectric parameters of an aged MV cable: A comparison of curve fitting, decision tree and artificial neural network methods. *Electric Power Systems Research*, *208*, 107892. https://doi.org/10.1016/j.epsr.2022.107892

Ashok, N., Soman, K. P., Samanta, M., Sruthi, M. S., Poornachandran, P., Devi V. G, S., & Sukumar, N. (2024). Polymer and Nanocomposite Informatics: Recent Applications of Artificial Intelligence and Data Repositories. *Advanced Machine Learning with Evolutionary and Metaheuristic Techniques*, 297-322. https://doi.org/10.1007/978-981-99-9718-3_12

Boukezzi, L., & Boubakeur, A. (2013). Prediction of mechanical properties of XLPE cable insulation under thermal aging: neural network approach. *IEEE Transactions on Dielectrics and Electrical Insulation*, *20*(6), 2125-2134. https://doi.org/10.1109/TDEI.2013.6678861

Cole, K. S., & Cole, R. H. (1941). Dispersion and absorption in dielectrics I. Alternating current characteristics. The Journal of chemical physics, 9(4), 341-351. https://doi.org/10.1063/1.1750906

Çanta, H., Mutlu, R., & Korkmaz Tan, R. (2024). Yeni Üretilen XLPE İzolasyonlu Tek Damarlı Bir Güç Kablosunun Kaçak Empedansının Hesabı. EMO Bilimsel Dergi, 14(1), 19-26.

Das, A. K., Chatterjee, S., Pradhan, A. K., Chatterjee, B., & Dalai, S. (2022). Estimation of moisture content in XLPE cable insulation using electric modulus. *IEEE Transactions on Dielectrics and*

Electrical Insulation, *29*(3), 1030-1037. https://doi.org/10.1109/TDEI.2022.3173485

Dessouky, S. S., El Faraskoury, A., El-Mekkawy, S., & El Zanaty, W. (2014). The Optimal Classification of Partial Discharge Defects within XLPE Cable by Using ANN and Statistical Techniques. Port-Said Engineering Research Journal, 18(2), 1-7. https://doi.org/10.21608/pserj.2014.45254

Du, Y., Geng, P., Song, J., Tian, M., & Pang, D. (2016, September). Influence of temperature and frequency on leakage current of XLPE cable insulation. In *2016 IEEE International Conference on High Voltage Engineering and Application (ICHVE)* (pp. 1-4). IEEE. https://doi.org/10.1109/ICHVE.2016.7800648

Ge, X., Given, M., & Stewart, B. G. (2022, September). Determining accelerated aging power cable spatial temperature profiles using Artificial Neural Networks. In *2022 IEEE International Conference on High Voltage Engineering and Applications (ICHVE)* (pp. 1-4). IEEE. https://doi.org/10.1109/ICHVE53725.2022.9961792

https://getdata-graph-digitizer.software.informer.com/ (Access date; June 02, 2023)

Gouda, O. E., & Matter, Z. (1992, August). Effect of the temperature rise on the XLPE dielectric properties. In *[1992] Proceedings of the 35th Midwest Symposium on Circuits and Systems* (pp. 95-98). IEEE. https://doi.org/10.1109/MWSCAS.1992.271325

Haykin, S. (1998). *Neural networks: a comprehensive foundation*. Prentice Hall PTR.

Hedir, A., Bechouche, A., Moudoud, M., Teguar, M., Lamrous, O., & Rondot, S. (2020). Experimental and predicted XLPE cable insulation properties under UVRadiation. *Turkish Journal of Electrical Engineering and Computer Sciences*, *28*(3), 1763-1775. 10.3906/elk-1910-58

Karhan, M., & Uğur, M. (2016). XLPE izoleli tek damarlı orta gerilim kablolarında elektrik alanının sulu ağaçlanmaya etkisinin incelenmesi. *Güç Sistemleri Konferansı (GSK2016), İstanbul*.

Karhan, M., Çakır, M. F., Arslan, Ö., Issı, F., & Eyüpoğlu, V. (2021). XLPE dielektrik malzemelerde elektrik alanının temas açısına ve damlacık şekline etkisi. *Gazi Üniversitesi Mühendislik Mimarlık Fakültesi Dergisi*, *36*(3), 1747-1760. https://doi.org/10.17341/gazimmfd.700362.

Lewis, C. D. (1982). Industrial and business forecasting methods: A practical guide to exponential smoothing and curve fitting, Butterworth-Heinemann.

Liang, P., & Bose, N. K. (1996). Neural network fundamentals with graphs, algorithms, and applications. *Mac Graw-Hill*.

Liu, Y., Wang, H., Zhang, H., & Du, B. (2022). Thermal aging evaluation of XLPE power cable by using multidimensional characteristic analysis of leakage current. *Polymers*, *14*(15), 3147. https://doi.org/10.3390/polym14153147

Moore, G. F. (Ed.), Electric cables handbook. Blackwell Science, UK, 1997, Blackwell Science, UK, 1997.

Öztürk, P., Alisoy, H., & Mutlu, R. (2019) Yapay Sinir Ağları Kullanarak İkili ve Üçlü Büküm Makinaların Ürettiği CAT 6A U/FTP Kabloların Parametrelerinin Tahmini ve Tahmin Edilen Sonuçların Karşılaştırılması. European Journal of Engineering and Applied Sciences, 2(2), 41-51.

Öztürk, P., Alisoy, H., & Mutlu, R. (2020). CAT 6A U/FTP Data Kablosunun Yüksek Frekans Parametrelerinin YSA ile Tahmin Modeli. *Nevşehir Bilim ve Teknoloji Dergisi*, 16-30. https://doi.org/10.17100/nevbiltek.728791

Rajagopalan, R., & Rajagopalan, P. (1996, January). Applications of neural network in manufacturing.

In *Proceedings of HICSS-29: 29th Hawaii International Conference on System Sciences* (Vol. 2, pp. 447-453). IEEE. DOI: 10.1109/HICSS.1996.495430

Shen, Z., Yang, L., Tang, H., & Lai, Y. (2021). Contact-free dielectric response measurement based on limit fitting by neural network. *IET Science, Measurement & Technology*, *15*(6), 499-507. https://doi.org/10.1049/smt2.12050

Slimani, F., Hedir, A., Moudoud, M., DURMUŞ, A., Amir, M., & Megherbi, M. (2021). Prediction of long-term physical properties of low density polyethylene (LDPE) cable insulation materials by artificial neural network modeling approach underenvironmental constraints. *Turkish Journal of Electrical Engineering and Computer Sciences*, *29*(5), 2437-2449. DOI: 10.3906/elk-2105-27 https://doi.org/10.3906/elk-2105-27

Selvamany, P., Varadarajan, G. S., Chillu, N., & Sarathi, R. (2022). Investigation of XLPE cable insulation using electrical, thermal and mechanical properties, and aging level adopting machine learning techniques. *Polymers*, *14*(8), 1614. https://doi.org/10.3390/polym14081614

Thue, W. A. (Ed.). (2017). *Electrical power cable engineering*. Crc Press.

Uydur, C. C., Arikan, O., & Kalenderli, O. (2018, September). The Effect of insulation defects on electric field distribution of power cables. In *2018 IEEE International Conference on High Voltage Engineering and Application (ICHVE)* (pp. 1-4). IEEE. DOI:10.1109/ICHVE.2018.8641936

Wang, X., Mo, F., Zhang, J., & Zhao, G. (2015). Study on the Parameters of Cole-Cole Model, International Conference on Advances in Mechanical Engineering and Industrial Informatics (AMEII 2015).

Wang, Y., Kang, N., Lin, J., Lu, S., & Liew, K. M. (2022). Cross-heating-rate prediction of thermogravimetry of PVC and XLPE cable insulation material: a novel artificial neural network framework. *Journal of Thermal Analysis and Calorimetry*, *147*(24), 14467-14478. https://doi.org/10.1007/s10973-022-11635-7

Zhang, Y., Wu, Z., Qian, C., Tan, X., Yang, J., & Zhong, L. (2020). Research on lifespan prediction of cross-linked polyethylene material for XLPE cables. *Applied Sciences*, *10*(15), 5381. https://doi.org/10.3390/app10155381

Zhou, T., Zhu, X., Yang, H., Yan, X., Jin, X., & Wan, Q. (2023). Identification of XLPE cable insulation defects based on deep learning. *Global Energy Interconnection*, *6*(1), 36-49. https://doi.org/10.1016/j.gloei.2023.02.004